New Folder Name Cryo Pump Infrared Shielding Considerations
T950087

DCC

CALIFORNIA INSTITUTE OF TECHNOLOGY

Laser Interferometer Gravitational Wave Observatory (LIGO) Project

To: Distribution
From: Dennis Coyne DC
Phone/FAX: 395-2034/304-9834

Refer to: LIGO-T950087-00-E
Date: 18 Nov 95

Subject: **Cryopump Infrared Shielding Considerations**

Background

PSI has proposed[1] to reduce the heat load (and LN_2 consumption rate) of the cryopumps through the use of cylindrical liners (shields) with low emissivity ($\varepsilon = 0.06$), diffuse surfaces on both sides of the cold surface, as indicated in Figure 1. PSI's calculations indicated a reduction in heat load to the cold surface of the long cryopump of approx. 33% is possible by using 1.52 m long liners on both sides of the long cryopump. The reduction in heat load is important in reducing the frequency of LN_2 tank refilling, reducing the size and expense of the LN_2 tank and reducing the cost of LN_2 during operation.

Figure 1: Cryopump Liners (Shields)

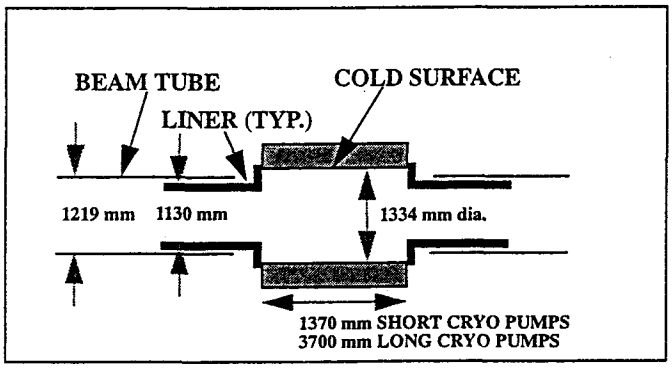

The "long" cryopumps have a 3.7 m long cylindrical cold surface and the "short" cryopumps have a 1.37 m long cylindrical cold surface. The internal diameters of the cold surfaces of both pumps are 1.334 m. PSI's current cryo pump design constrains the maximum diameter of the liners to be 1.13 m (PSI drawing V049-4-004, Rev. P1). The lengths of the liners for the cryo pumps are constrained by the placement of the adjacent gate valves; There appears to be some freedom in locating these gate valves relative to the cryo pump so as to achieve liner lengths on the order of 1 to 2 meters in length.

1. Process Systems International (PSI), LIGO Vacuum Equipment Preliminary Design, Vol. 1, Attachment 1.4, "80K Pump Performance", PSI-VE001AA1A01, 19 Jun 95.

Cryopump Infrared Shield Performance Analysis

An independent analysis of the effectiveness of the cryopump liner was undertaken due to concerns about the validity of two assumptions by PSI:

1) the entire beam tube (including the tube in proximity to the shield) acts like a black body, and
2) one can obtain a surface which behaves like a diffuse (Lambertian) IR reflector with low emissivity

The Lambertian characteristic of the surface is crucial; If the surface behaved as a specular reflector, then it would in essence simply mirror the black body of the beam tube to the cold surface and it would have no effect.

As reported previously[1], a view factor and radiation balance calculation[2] confirmed PSI's calculations of the mitigation in radiative heat load to the cold surface due to diffusive, low emissivity liners with the following parameters:

1) long cryopump (3.7 m cold surface length, and 1.2 m diameter[3])
2) beam tube emissivity of 0.5
3) liner emissivity of 0.06 (diffuse)
4) liner length of 1.52 m

These calculations were based upon view factors for a coarse discretization of the geometry (i.e. a single view factor for each component). The calculations confirm that the simplification of treating the beam tube as a black body is reasonable.

Further calculations have determined the effectiveness of the liners for the revised cryo pump diameter with a finer discretization to account for the gradient in radiosity. In the analysis the geometry of Figure 1 was approximated by assuming that the beam tube, liners and cryopump cold surface are all at the same diameter (the diameter of the beam tube, 1.2 m). The analysis will be updated for a subsequent revision of this memorandum; I did not want to delay release of this memo and the discussion which will ensue of the implications of the integration of the liner and laser light baffles. In addition, the analysis does not account for the interaction of the liners with the laser light baffles (to be discussed in the next section). On the basis of this analysis, the performance of the infrared shields for the long and short cryopumps as a function of shield length and parameterized by shield emissivity, are given in Figures 2 and 3 respectively. Although the performance will change somewhat when the diameters are revised, the results will not be substantially different.

Further extension to the radiative transport analysis of the liner effectiveness to account for the different diameters of the tube, liner and cold surface as well as inclusion of the laser light baffles, can be accomplished readily. As an alternative which would permit analysis of more complex geometries, I attempted to use the TMG module within the I-Deas Master Series 2 computer aided

---

1. Coyne, D., "Cryo Pump Shield Performance Analysis", e-mail to M. Zuker, A. Lazzarini and J. Worden, 2 Nov 95.
2. Siegel, H. and Howell, J., Thermal Radiation Heat Transfer, 2nd ed., McGraw Hill, 1972, pp.236-248.
3. The diameter of the cryopumps was 1.2 m at the time of PSI's initial PDR (June 95). The diameter has since been increased to 1.334 m based upon laser light baffling requirements as discussed in LIGO-L950593-01-E.

design and analysis package for analysis of specular as well as diffuse components of reflection. Although TMG is capable of handling combined diffuse and forward specular reflections which are independent of incidence angle, TMG cannot handle retro-reflection. Given that suitable nearly Lambertian surfaces are obtainable (as discussed in the next section), TMG may be adequate for any further analysis with more complex geometry (if necessary). Inclusion of a complete BRDF characterization in the analysis would require another code, perhaps TRASYS or CODE-V.

Figure 2: Long Cryopump Liner (Infrared Shield) Performance (for liner emissivities of 0.06 and 0.10)

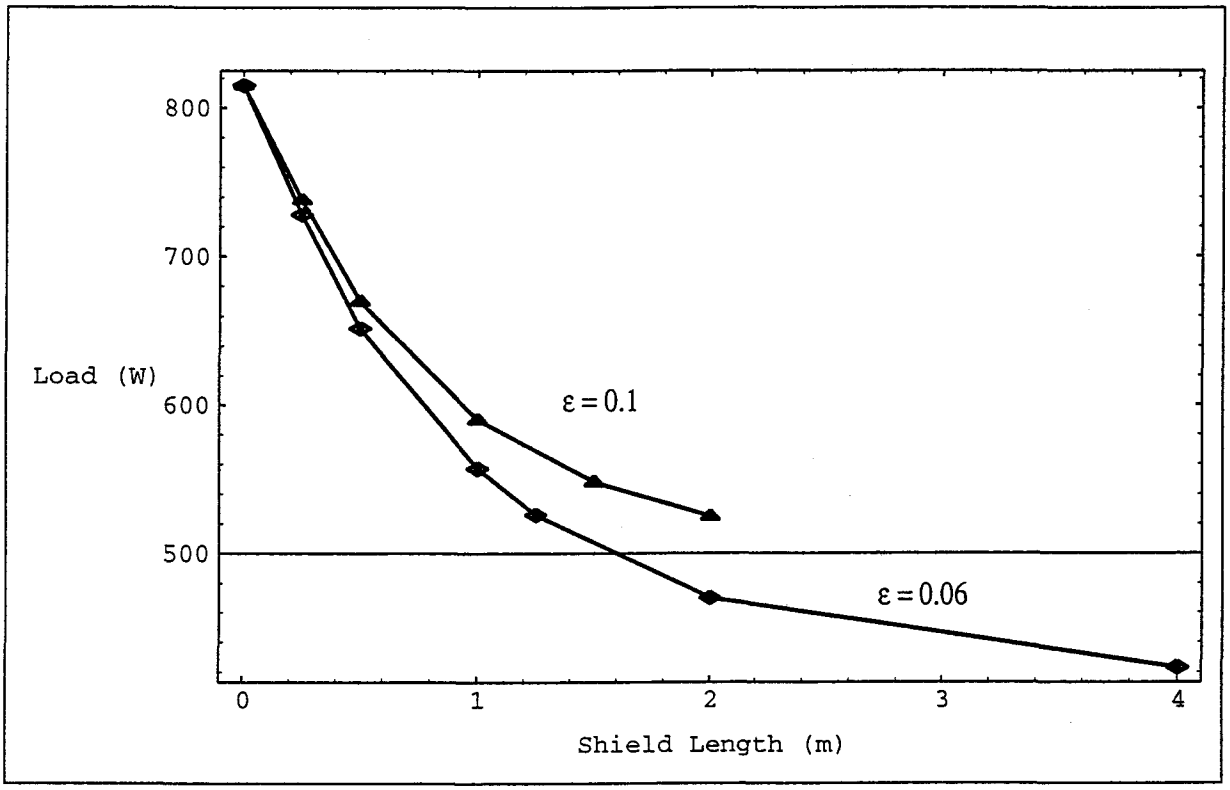

Figure 3: Short Cryopump Liner (Infrared Shield) Performance (for liner emissivities of 0.06, 0.10 and 0.20)

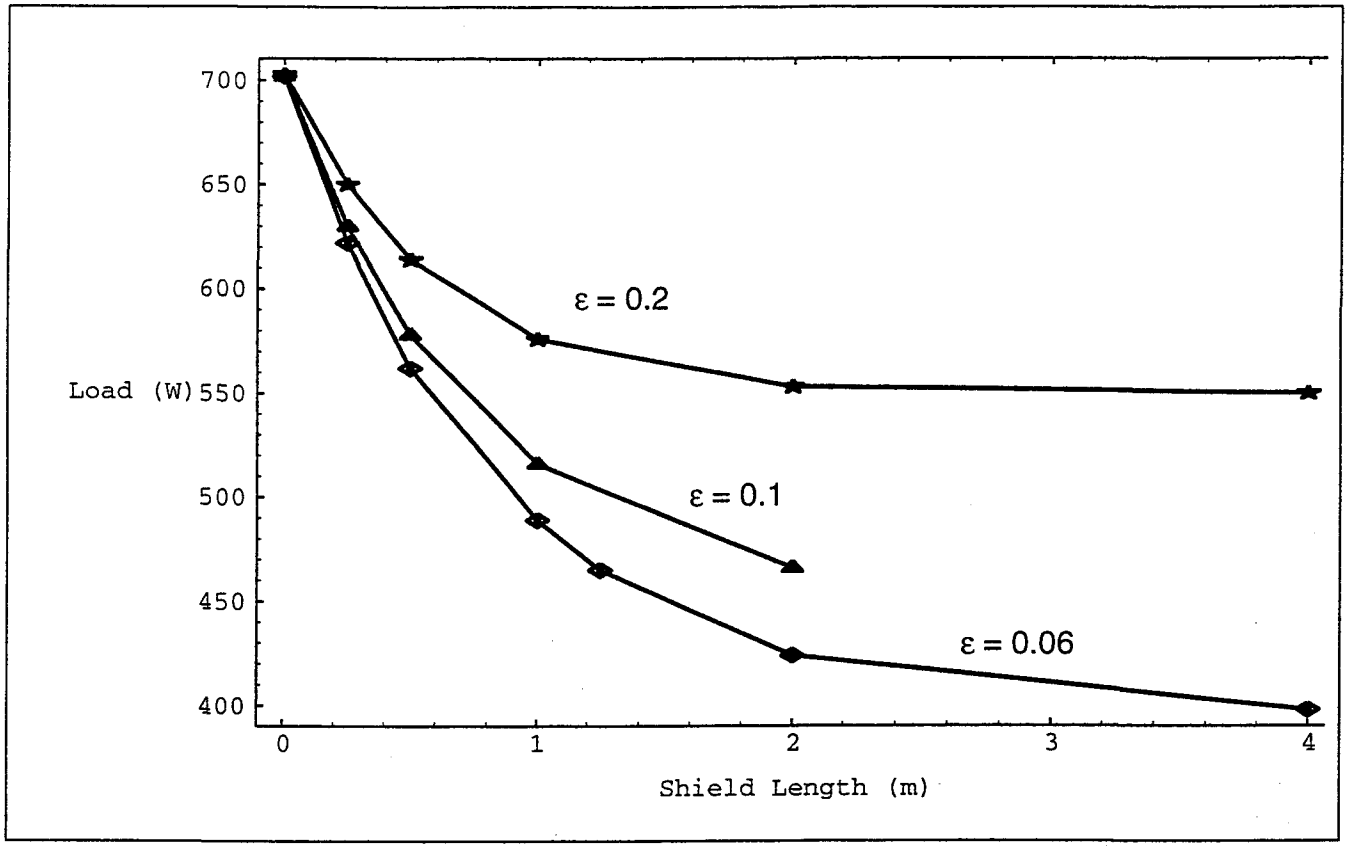

Diffuse Infrared Shield Material

A quick check in the literature and discussions with Dr. Bob Breault (of Breault Research Organization, Inc.) indicates that Flame Sprayed Aluminum (FSA) or gold on FSA can meet the requirements for a low emissivity, diffuse reflector in the infrared. Attached are two references[1,2], with BRDF measurements on bare FSA and gold coated FSA. In the second reference, the MIL-STD used in the fabrication of the FSA surface is cited. The directional-hemispherical reflectance at 10.6 microns is approximately 0.85 for bare FSA and 0.95 for gold coated FSA. Both have very flat BRDFs indicating diffuse (Lambertian) behavior for low angles of incidence (as indicated in the attached). As the angle of incidence increases, these materials deviate more from a perfect Lambertian surface with a slight retro-component of reflection and a slight forward scatter (specular) component. However, the deviations from ideal Lambertian behavior are slight (about +/- 15%). The retro-reflection helps in reducing the infrared flux from the beam tube, but increases

1. Oppenheim, U., Turner, M., and Wolfe, W., "BRDF Reference Standards for the Infrared", Infrared Phys. Technol., Vol. 35, No. 7, pp. 873-879, 1994.
2. Brennan, W. (Hughes Electro-Optical & Data Systems Group) to Breault, R., letter with attached data on BRDF of flame sprayed aluminum at 5 deg. angle of incidence and 3 wavelengths (1.06, 3.39 and 10.6 microns), 23 Oct 91.

the coupling of emission from the absorptive side of the laser light baffles placed adjacent to the cold surface.

Considerations Related to the Integration of Laser Light Baffles and Infrared Shields

The minimum diameter of the LN_2 trap based upon considerations of optical shielding of the cold surface from view of the test masses has been addressed in a memorandum by Albert Lazzarini[1]. This analysis does not account for the presence of the liners. For the same reasons outlined in this memorandum, the shields (or liners) should not be visible to the test masses, as indicated in Figure 5 (a to-scale drawing).

Stan Whitcomb has pointed out that PSI's proposal to use a diffusive shield in order to reduce the thermal load on the cryo-pump extends the effective length of the cryo-pump considerably resulting in some special considerations in combined IR and optical shielding. The dimensions indicated in the Figure 5 are for the most restrictive baffling situation, i.e. the short cryopumps at the mid- and end-stations. The diameters of the cryopump and its shields result in restricting the maximum length of the liners to about 0.8 m and 1.0 m (for the liner closest to, and farthest from, the test mass respectively) IF no laser light baffles are placed within the infrared liners.

Due to the asymmetric nature of the problem, the two baffles placed between the cold surface and the test mass (Figure 5) serve to absorb laser light on one side and act as a low emissivity infrared radiator on the opposite side. The baffle placed on the side of the cold surface most distant from the test mass (and used to block direct view of the far liner) must be absorptive at the laser wavelength (and therefore absorptive in the infrared as well). Consequently, this baffle will compromise the ideal performance of the liners. However, the view factor from the cold surface to this baffle is not large (as can be seen from the scale drawing, Figure 4). A single baffle to block view of the cold surface and the far liner is impractical (diameter > 1.45 m for a liner of only 0.5 m in length).

An alternative to the use of diffuse liners (suggested by Stan Whitcomb), is to use a retro-reflection surface, as indicated in Figure 4. The cold surface would see itself and the self-emission of the (low emissivity) surface of the liner; The infrared emission of the beam tube would be retro-

1. Lazzarini, A.,"Determination of the minimum LN_2 trap inner diameter needed to shield it from direct line of sight from a test mass", LIGO-L950593-01-E, 2 Nov 95.

reflected back down the tube. The performance of this approach is yet to be determined.

Figure 4: Cryopump Liners (Shields)

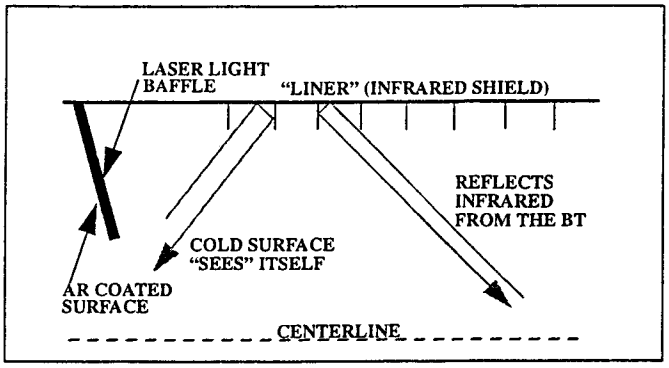

In either approach for infrared shielding, the laser light baffles adjacent to the cryo pumps would have to be treated differently from the baffles in the beam tube. Stan suggests an broad-band AR coating (from 1 to 10 microns).

DCC:dcc

Attachments:

1) Drawing D95~~xxxx~~0162-SK (11/18/95), Cryopump Liner and Baffle Considerations
2) Cryopump Radiant Interchange Analysis (derivation and Mathematica Notebook)
3) Oppenheim, U., Turner, M., and Wolfe, W., "BRDF Reference Standards for the Infrared", Infrared Phys. Technol., Vol. 35, No. 7, pp. 873-879, 1994.
4) Brennan, W. (Hughes Electro-Optical & Data Systems Group) to Breault, R., letter with attached data on BRDF of flame sprayed aluminum at 5 deg. angle of incidence and 3 wavelengths (1.06, 3.39 and 10.6 microns), 23 Oct 91.

Distribution:

W. Althouse	F. Raab	G. Stapfer	J. Worden
M. Coles	G. Sanders	K. Thorne	W. Young
B. Barish	D. Shoemaker	R. Vogt	M. Zucker
D. Jungwirth	A. Sibley	R. Weiss	Chronological File
A. Lazzarini	R. Spero	S. Whitcomb	Document Control Center

NOTES: (UNLESS OTHERWISE SPECIFIED)

NOTE: POTENTIAL INTERFERENCE OF LINERS WITH GATE VALVES (see PSI Dwgs V049-4-005, rev.P1 and V049-5-004, rev.P1)

REV	DESCRIPTION OF CHANGE	SHEETS AFFECTED	APPROVAL	DATE
SK				

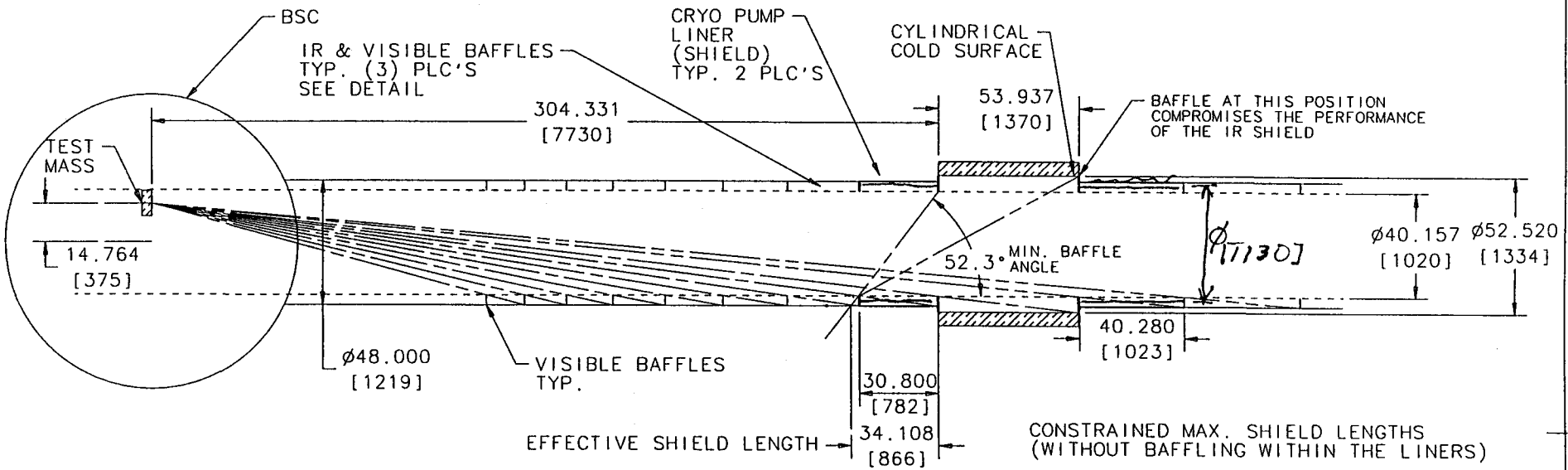

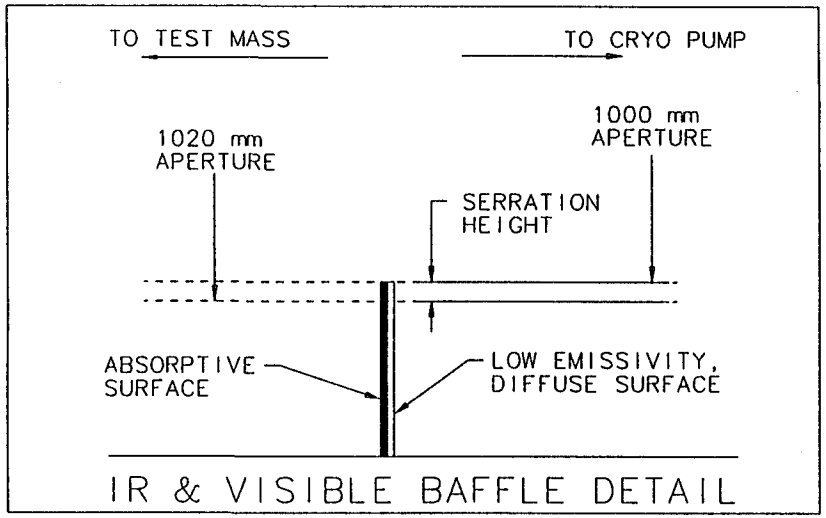

IR & VISIBLE BAFFLE DETAIL

QTY REQD	FSCM NO	PART OR IDENTIFYING NO	NOMENCLATURE OR DESCRIPTION	MATERIAL SPECIFICATION	ITEM NO

PARTS LIST

UNLESS OTHERWISE SPECIFIED DIMENSIONS ARE IN ft-in (mm) TOLERANCES ARE: FRACTIONS DECIMALS

DO NOT SCALE DRAWING

MATERIAL

FINISH

APPROVALS	DATE
DRAWN D. Coyne	11/22/95
CHECKED	

LIGO CALIFORNIA INSTITUTE OF TECHNOLOGY MASSACHUSETTS INSTITUTE OF TECHNOLOGY

TITLE: CRYO PUMP LINER AND BAFFLE CONSIDERATIONS

DWG NO. D950162 REV SK

SCALE SHEET 1 OF 1

Figure 5.

CRYO PUMP RADIANT INTERCHANGE

D. LeCayne 10/30/95

Finite Area Approximation:

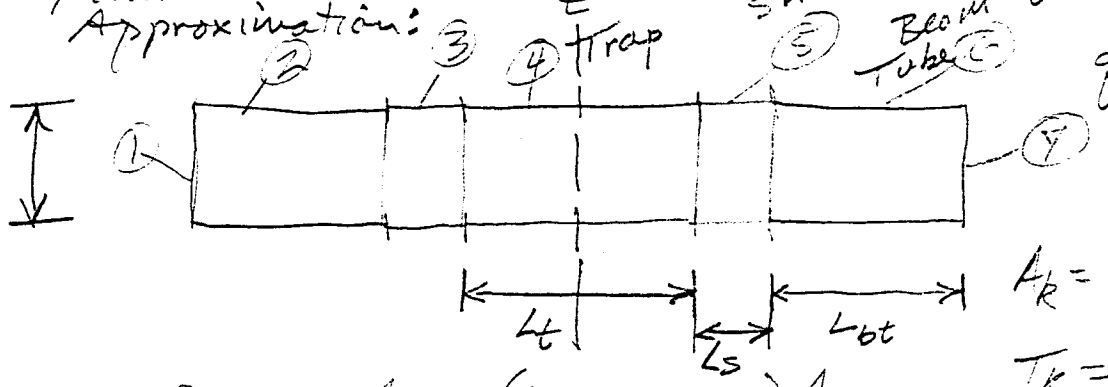

(Lower shield)

q_o = radiosity (outgoing radiation)

q_i = incoming radiation

A_k = Surface area of k^{th} surface

T_k = Temperature of k^{th} surface

① $Q_k = q_k A_k = (q_{o,k} - q_{i,k}) A_k$

② $q_{o,k} = \epsilon_k \sigma T_k^4 + \rho_k q_{i,k} = \epsilon_k \sigma T_k^4 + (1-\epsilon_k) q_{i,k}$

$$A_k q_{i,k} = A_1 q_{o,1} F_{1-k} + A_2 q_{o,2} F_{2-k} + \dots + A_j q_{o,j} F_{j-k} + \dots + A_k q_{o,k} F_{k-k} + \dots + A_N q_{o,N} F_{N-k}$$

or

③ $$q_{ik} = \sum_{j=1}^{N} F_{k-j} q_{o,j}$$

(using the config factor reciprocity relation $A_1 F_{1-k} = A_k F_{k-1}$)

from ②:

$$q_{i,k} = \left(\frac{1}{1-\epsilon_k}\right)\left(q_{o,k} - \epsilon_k \sigma T_k^4\right)$$

combining with ①:

$$Q_k = A_k \left[q_{o,k} + \left(\frac{1}{1-\epsilon_k}\right)\left(\epsilon_k \sigma T_k^4 - q_{o,k}\right)\right]$$

④ $$\boxed{Q_k = A_k \left(\frac{\epsilon_k}{1-\epsilon_k}\right)\left[\sigma T_k^4 - q_{o,k}\right]}$$

combining ① and ③:

⑤ $$\boxed{Q_k = A_k \left(q_{o,k} - \sum_{j=1}^{N} F_{k-j} q_{o,j}\right)}$$

Equating (2) and (3):

$$q_{o,k} - \sum_{j=1}^{N} F_{k-j}\, q_{o,j} = \left(\frac{\epsilon_k}{1-\epsilon_k}\right)\left[\sigma T_k^4 - q_{o,k}\right]$$

$$q_{o,k} - (1-\epsilon_k)\sum_{j=1}^{N} F_{k-j}\, q_{o,j} = \epsilon_k \sigma T_k^4$$

(6) $$\boxed{\sum_{j=1}^{N}\left[\delta_{kj} - (1-\epsilon_k)F_{k-j}\right] q_{o,j} = \epsilon_k \sigma T_k^4}$$

(7) $$[a]\{q_o\} = \{c\}$$

(8) $$\{q_o\} = [a]^{-1}\{c\}$$

Use

(5) $$Q_k = A_k\left(q_{o,k} - \sum_{j=1}^{N} F_{k-j}\, q_{o,j}\right)$$

- to project out the net heat balance at each surface

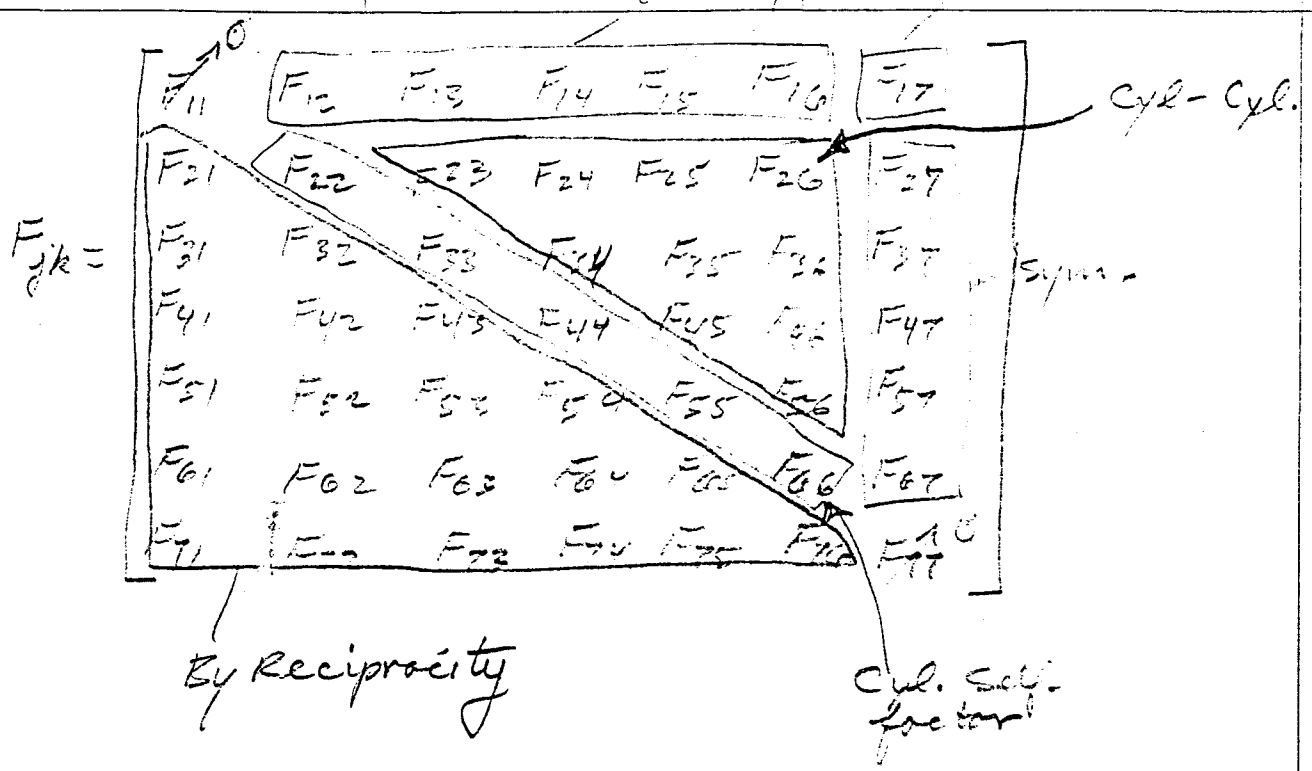

Discretization of the component geometries in straight forward:

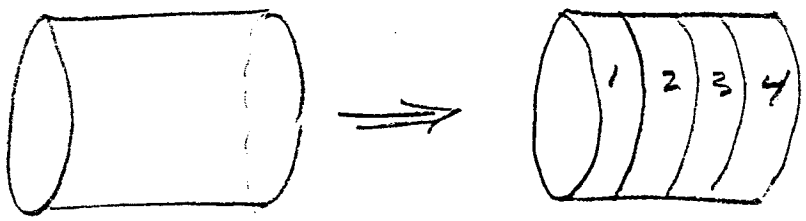

CRYO PUMP RADIANT INTERCHANGE

Cryo Pump Properties

Component Dimensions

In[2790]:=

```
Dia = 1.22;      (* m *)
Ltrap = 3.7;     (*large cryo-pump, m *)
Lshield = 1.5;   (* m *)
Lbt = 20;        (* m *)
```

In[2794]:=

```
radius = Dia/2;
L = Ltrap + 2 (Lshield + Lbt);      (* overall length, m *)
```

Component Emissivities

In[2796]:=

```
eend = 0.9;          (* emissivity of the bt ends *)
ebt = 0.5;           (* emissivity of the beam tube *)
eshield = 0.06;      (* emissivity of the shields *)
etrap = 1.0;         (* emissivity of the cold trap *)
```

Component Temperatures (K)

In[2800]:=

```
Tend = 295;
Tbt = 295;
Tshield = 295;
Ttrap = 80;
```

Cryo Pump Model Parameters

Segmentation

In[2804]:=

```
ntrap = 10;      (* number of segments for the cold trap surface *)
nshield = 10;    (* number of segments for each shield surface *)
nbt = 20;        (* number of segments for each beam tube surface *)
n = 2 + 2 (nbt + nshield) + ntrap
```

Out[2807]=

72

Segmented Surface Area, Position, Length, Emissivity & Temperature

In[2808]:=

```
A = Table[0,{n}];
emiss = A;
T = A;
x = A;
s = A;
A[[1]] = Pi Dia^2/4;
A[[n]] = A[[1]];
emiss[[1]] = eend;
emiss[[n]] = emiss[[1]];
T[[1]] = Tend;
T[[n]] = T[[1]];
x[[1]] = 0;
x[[n]] = L;
s[[1]] = 0;
s[[n]] = 0;
```

In[2823]:=

```
As = Pi Dia Lbt/nbt;
es = ebt;
Ts = Tbt;
ss = Lbt/nbt;
Do [
   A[[i]] = As;
   emiss[[i]] = es;
   T[[i]] = Ts;
   s[[i]] = ss;
   x[[i]] = x[[i-1]] + s[[i-1]];
   A[[i+nbt+ntrap+2 nshield]] = As;
   emiss[[i+nbt+ntrap+2 nshield]] = es;
   T[[i+nbt+ntrap+2 nshield]] = Ts;
   s[[i+nbt+ntrap+2 nshield]] = ss;
   x[[i+nbt+ntrap+2 nshield]] = x[[i]] + Lbt + Ltrap + 2 Lshield,
   {i,2,nbt+1}
];
As = Pi Dia Lshield/nshield;
es = eshield;
Ts = Tshield;
ss = Lshield/nshield;
Do [
   A[[i]] = As;
   emiss[[i]] = es;
   T[[i]] = Ts;
   s[[i]] = ss;
   x[[i]] = x[[i-1]] + s[[i-1]];
   A[[i+nshield+ntrap]] = As;
   emiss[[i+nshield+ntrap]] = es;
   T[[i+nshield+ntrap]] = Ts;
   s[[i+nshield+ntrap]] = ss;
   x[[i+nshield+ntrap]] = x[[i]] + Lshield + Ltrap,
   {i,nbt+2,nbt+nshield+1}
];
As = Pi Dia Ltrap/ntrap;
es = etrap;
Ts = Ttrap;
ss = Ltrap/ntrap;
Do [
   A[[i]] = As;
   emiss[[i]] = es;
   T[[i]] = Ts;
   s[[i]] = ss;
   x[[i]] = x[[i-1]] + s[[i-1]],
   {i,nbt+nshield+2,nbt+nshield+ntrap+1}
];
```

View Factors

In[2838]:=

```
F = Table[0,{n},{n}];
```

Disk-Disk View Factors

N.B.: Concentric, r1 and r2 are radii , h = distance between disks

In[2839]:=

```
Fdd[r1_,r2_,h_]:= If[h == 0, 1,
With[{X=1+(1+(r2/h)^2)/(r1/h)^2}, 1/2 (X - Sqrt[X^2 - 4
(r2/r1)^2])]];
```

Left End Disk(1) - Right End Disk(n):

In[2840]:=

```
F[[1,n]]=Fdd[Dia/2,Dia/2,L];
```

Disk-Interior Cylinder View Factors

N.B.: Concentric, r1 = disk radius, r2 = cylinder radius, r1 <= r2, h1 = distance from disk to near end of cyliner, h2 = distance from disk to far end of cylinder

In[2841]:=

```
Fdc[r1_,r2_,h1_,h2_]:=Fdd[r1,r2,h1] - Fdd[r1,r2,h2];
```

Left End Disk(1) - Cylindrical Segments (2->n-1) and by symmetry, Cylindrical Segments (2->n-1) - Right End Disk(n):

In[2842]:=

```
Do [
   F[[1,i]]=Fdc[radius,radius,x[[i]],x[[i]]+s[[i]]];
   j = n-i+1;
   F[[j,n]]=F[[1,i]] A[[n]]/A[[j]],
   {i,2,n-1}
];
```

Interior Cylinder Self-View Factors

N.B.: r = radius, l = cylinder length

In[2843]:=

```
Fcself[r_,l_]:=1 - (r/l) Fdc[r,r,0,l];
```

☐ Cylindrical Segments (i) - Cylindrical Segments (i), for i={2,n-1}:

In[2844]:=

```
Do [
   F[[i,i]] = Fcself[radius,s[[i]]],
   {i,2,n-1}
];
```

■ Interior Equal-Diameter Concentric Cylinder View Factors

N.B.: r = radius, l1 = cylinder 1 length, l2 = cylinder 2 length, h = separation distance

In[2845]:=

```
Fceq[r_,l1_,l2_,h_]:=(Fdc[r,r,h,l1+h] - Fdc[r,r,l2+h,l2+l1+h]) (r/(2 l
```

☐ Cylindrical Segments (i) - Cylindrical Segments (j), for i,j={2,n-1}:

In[2846]:=

```
Ftemp=Table[0,{n},{n}];
```

In[2847]:=

```
Do [
   Do [
      F[[i,j]]=Fceq[radius,s[[i]],s[[j]],x[[j]]-x[[i]]-s[[i]]];
      Ftemp[[i,j]]=F[[i,j]],
      {j,i+1,n-1}
   ],
   {i,2,n-2}
];
```

■ Reciprocity

In[2848]:=

```
Do[
  Do [
    F[[i,j]] = F[[j,i]] A[[j]]/A[[i]],
  {j,1,i-1}],
{i,2,n}];

Do[
  Print[Sum[F[[i,j]],{j,1,n}]],
{i,1,n}];
```

Radiant Exchange Solution

In[2849]:=

```
one = Table[1,{n}];
a = IdentityMatrix[n] - Dot[DiagonalMatrix[(one - emiss)],F];
```

In[2851]:=

```
stefanBoltzmann = 5.6696 10^-8;(* W/m^2/K^4 *)
b = stefanBoltzmann emiss T^4;
```

In[2853]:=

```
qo = Inverse[a].b;
```

In[2854]:=

```
q = qo - F.qo //N;
```

In[2855]:=

```
Q = Dot[DiagonalMatrix[A],(qo - F.qo)] //N;
```

In[2856]:=

```
Qends = Q[[1]] + Q[[n]]
```

Out[2856]=

```
0.302877
```

In[2857]:=

```
Qbts = Sum[Q[[i]],{i,2,nbt+1}] +Sum[Q[[i]],{i,nbt+ntrap+2
nshield+2,n-1}]
```

Out[2857]=

```
363.647
```

In[2858]:=

```
Qshields = Sum[Q[[i]],{i,nbt+2,nbt+nshield+1}]
+Sum[Q[[i]],{i,nbt+nshield+ntrap+2,nbt+ntrap+2 nshield+1}]
```

Out[2858]=

```
138.878
```

In[2859]:=

```
Qtrap = Sum[Q[[i]],{i,nbt+nshield+2,nbt+nshield+ntrap+1}]
```

Out[2859]=

```
-502.828
```

In[2860]:=

```
xmid = x + s/2 - L/2;
```

In[2861]:=

```
ListPlot[Transpose[Partition[Join[xmid,q],n]],PlotJoined-
>True,PlotRange->{{-5,5},All}];
```

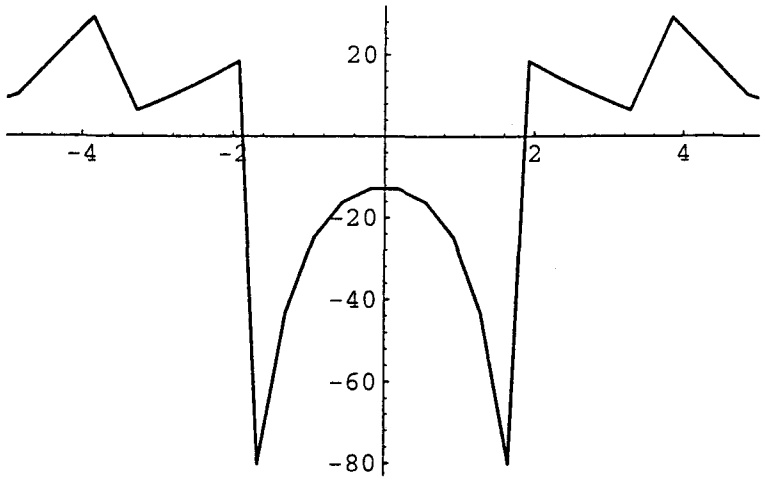

In[2862]:=

```
ListPlot[Transpose[Partition[Join[xmid,Q],n]],PlotJoined-
>True,PlotRange->{{-10,10},All}];
```

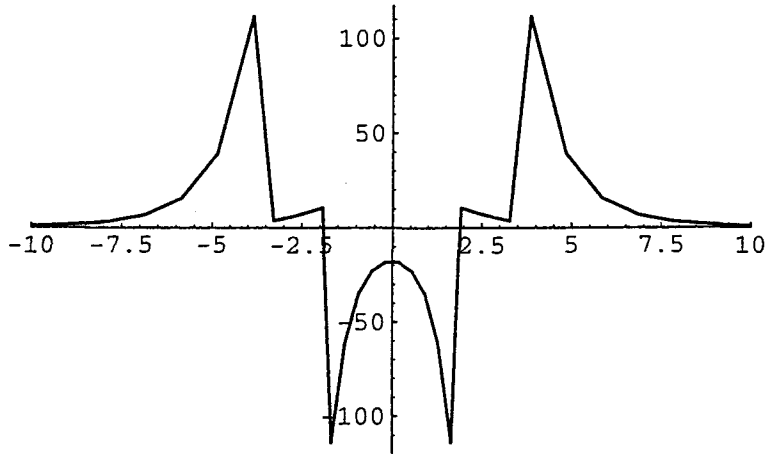

Tabulated Results

Long Cryo-Pump

1.2 m diameter
3.7 m long cold trap
nominally 1.52 m long shields (liners)
trap emissivity = 1.0 (ice)
shield emissivity = 0.06 (diffuse)
beam tube model length = 20 m

shield emissivity = 0.06
nbt = 20
nshield = 5
ntrap = 10
n = 62
Qtrap = 504 W
q (W/m^2) vs Xmid (m) :

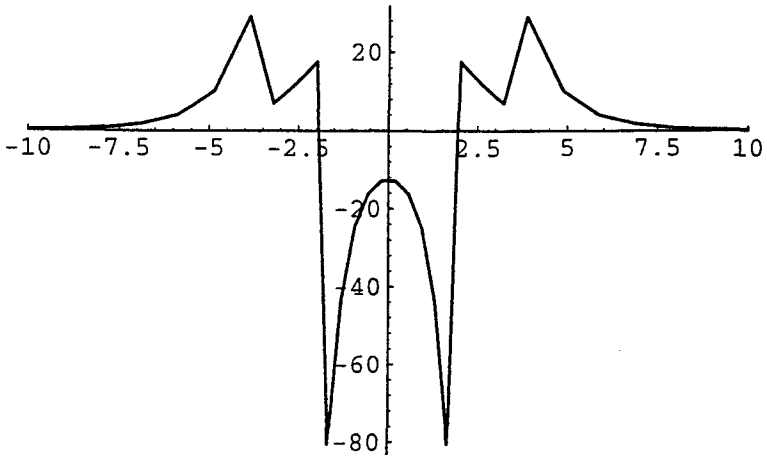

shield emissivity = 0.5
nbt = 20
nshield = 5
ntrap = 10
n = 62
Qtrap = 817 W (823 W when Lshield == 3 m)
q (W/m^2) vs Xmid (m) :

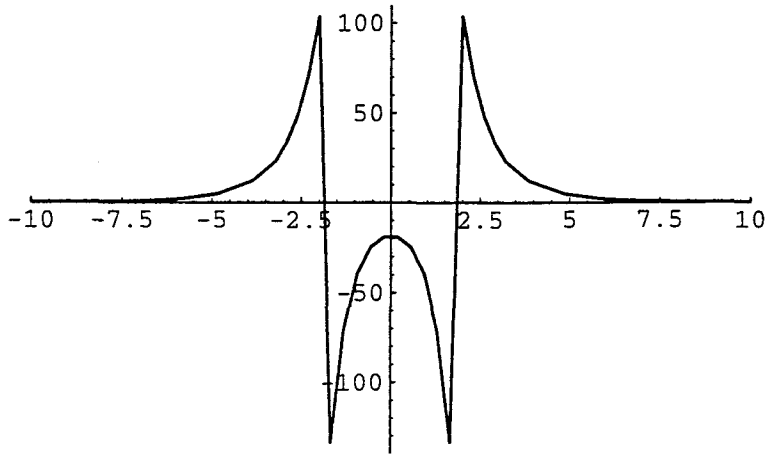

In[2863]:=

```
Needs["Graphics`MultipleListPlot`"]
```

Used nshield = 10, for a no-shield resulting Q = 815 W in the following sensitivity calculations to shield emissivity and length:

In[2864]:=

```
emissShield = {0.06, 0.10};
```

In[2865]:=

```
Qlong = {{{0,815}, {0.25,728}, {0.5,652}, {1.0,557},
{1.25,526}, {2,470}, {4,423}},
{{0,815},{0.25,738}, {0.5,670}, {1,590}, {1.5,548}, {2,525}}};
```

In[2866]:=

```
MultipleListPlot[Qlong[[1]],Qlong[[2]],PlotJoined-
>True,PlotRange->All,LineStyles-
>{{},{Dashing[{0.02,0.01}]},{Dashing[{0.03,0.01,0.01,0.01}]}},
Frame->True, RotateLabel->False, FrameLabel->{"Shield Length
(m)","Load (W)"}];
```

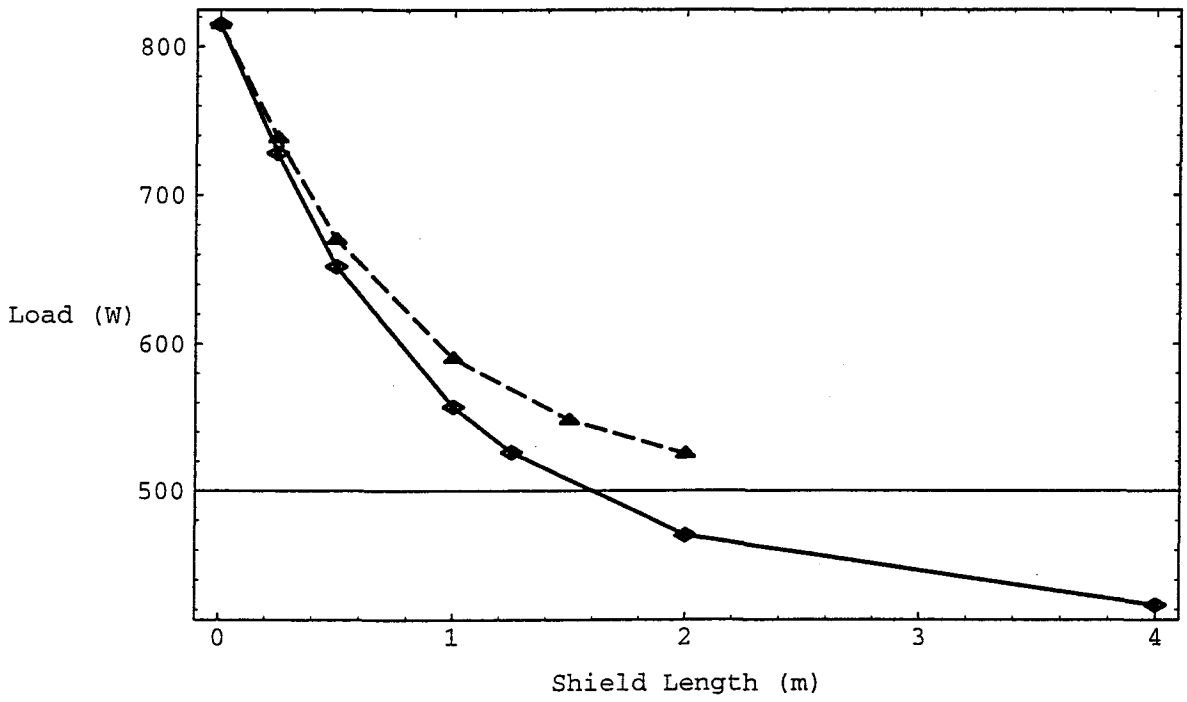

Heat load (W) on the inner surface of the cryo-pump (cold trap) for the "long" (3.7 m) cryo-pump, as a function of shield length (m) parameterized by emissivity (0.06, 0.10 and 0.20).

Short Cryo-Pump

1.2 m diameter
1.2 m long cold trap
1 m long shields (liners)
trap emissivity = 1.0 (ice)
shield emissivity = 0.06 (diffuse)
beam tube model length = 10 m

shield emissivity = 0.06
nbt = 20
nshield = 5
ntrap = 10
n = 62
Qtrap = 489 W
q (W/m^2) vs Xmid (m) :

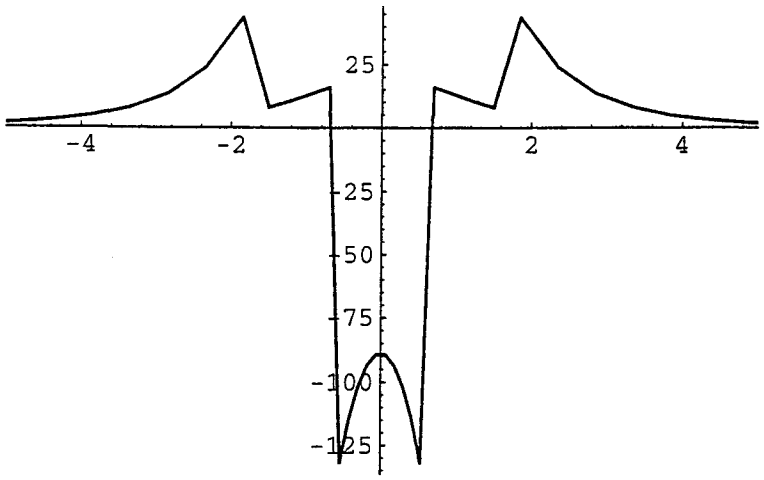

shield emissivity = 0.5
nbt = 20
nshield = 5
ntrap = 10
n = 62
Qtrap = 702 W (when Lshield == 1 m)
Qtrap = 708 W (when Lshield==3 m)
q (W/m^2) vs Xmid (m) :

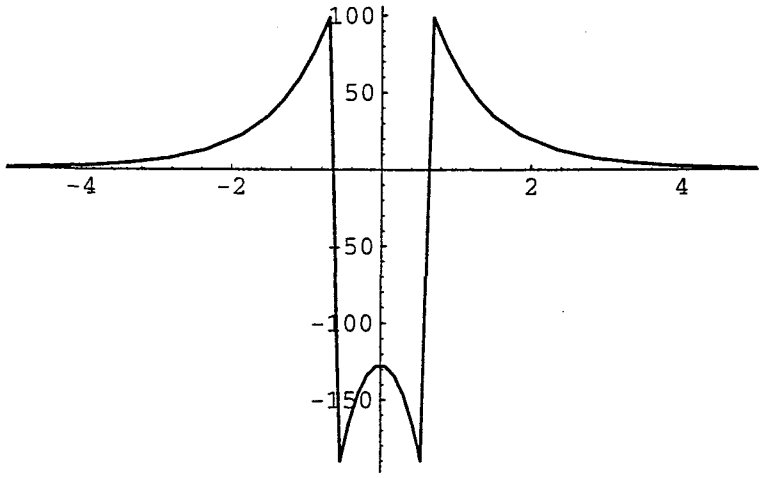

Note: Used 10 segments for the shield when the emissivity of the shield was set to 0.2

In[2867]:=

```
emissShield = {0.06, 0.10, 0.20};
```

In[2868]:=

```
Qshort = {{{0,702}, {0.25,622}, {0.5,562}, {1.0,489},
{1.25,465}, {2,424}, {4,398}},
{{0,702},{0.25,630}, {0.5,578}, {1,516}, {2,466}},
{{0,703}, {0.25,650}, {0.5,614}, {1,576}, {2,553}, {4,550}}};
```

In[2869]:=

```
MultipleListPlot[Qshort[[1]],Qshort[[2]],Qshort[[3]],PlotJoined
->True,PlotRange->All,LineStyles-
>{{},{Dashing[{0.02,0.01}]},{Dashing[{0.03,0.01,0.01,0.01}]}},
Frame->True, RotateLabel->False, FrameLabel->{"Shield Length
(m)","Load (W)"}];
```

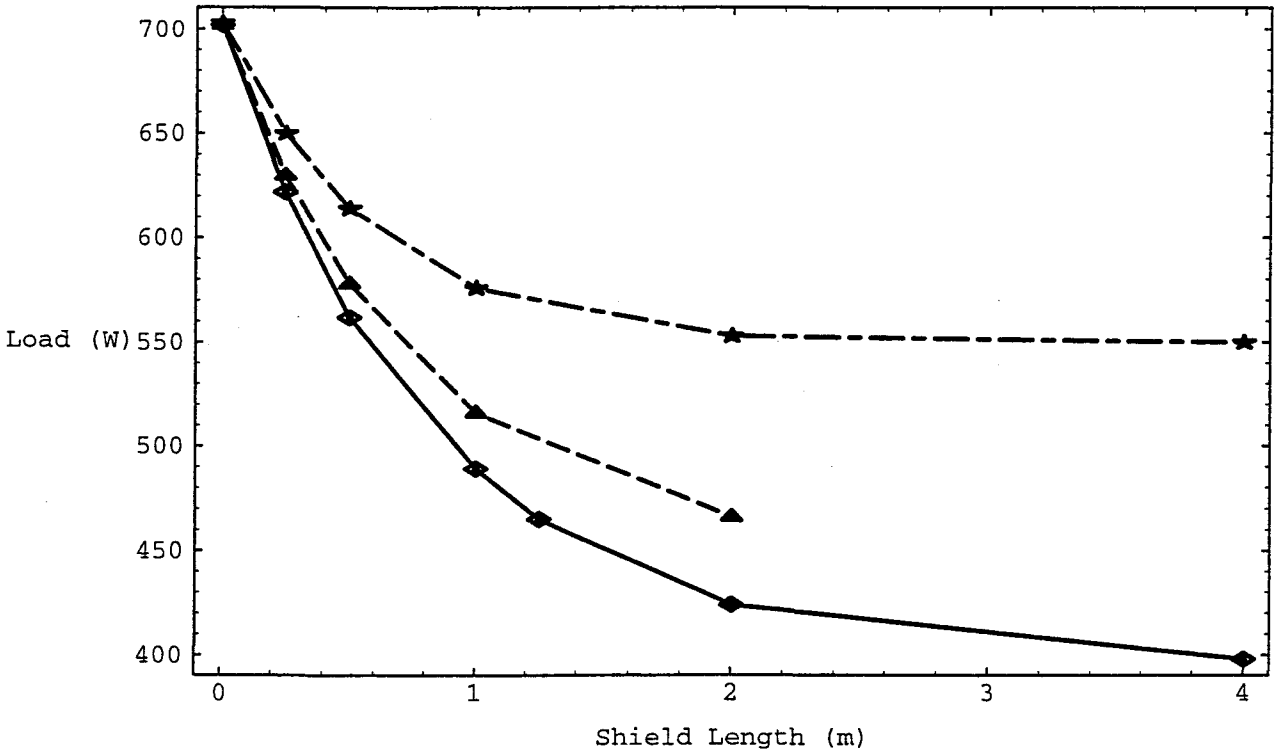

Heat load (W) on the inner surface of the cryo-pump (cold trap) for the "short" (1.2 m) cryo-pump, as a function of shield length (m) parameterized by emissivity (0.06, 0.10 and 0.20).

D. Coyne

Pergamon

1350-4495(94)00034-4

Infrared Phys. Technol. Vol. 35, No. 7, pp. 873–879, 1994

1350-4495/94 $7.00 + 0.00

BRDF REFERENCE STANDARDS FOR THE INFRARED

URI P. OPPENHEIM,† MARY G. TURNER and W. L. WOLFE
Optical Sciences Center, University of Arizona, Tucson, AZ 85721, U.S.A.

(Received 24 April 1994)

Abstract—A comparison between various recommended reference standards of diffuse reflectance in the IR is presented. It is shown that at a wavelength of 10.6 μm sulfur is the most Lambertian of the tested samples, although its powdery consistence makes it less suitable for use as a standard. Flame sprayed aluminum, with or without gold coating, also approaches a Lambertian surface and is suitable for use as a standard for BRDF measurements at 10.6 μm. Results for the BRDF of sulfur, gold-coated sandpaper, a commercial diffuse gold surface (by Labsphere) and flame sprayed aluminum are presented.

INTRODUCTION

Round Robin studies of the Bidirectional Reflectance Distribution Function (BRDF) of surfaces in the infrared[1,2] have proved the need for better reference standards and improved measurement techniques in this region of the spectrum. The latest report[3] shows differences in BRDF values of up to 50% between laboratories. There is a need for highly diffuse surfaces which are also highly reflecting in the IR and at the same time are sturdy and reproducible.

The present study is a comparison between several candidates for diffuse standards made with the AZSCAT [Arizona Scatterometer[4]] situated in the Optical Sciences Center of the University of Arizona. The source of radiation was a chopped cw CO_2 laser, polarized in the vertical direction which was always normal to the plane of incidence of the sample. The samples available for this study were sulfur, gold-coated sandpaper, a commercial diffuse gold surface and flame sprayed aluminum (bare and gold-coated). Angles of incidence were chosen at 10, 30, 45 and 60°. BRDF measurements for all these samples are presented.

Although no specular reflectance peak was observed for these samples (except the commercial sample), a distinct "retro" effect was observed, showing a hump in the BRDF curve at a backscatter angle equal to the angle of incidence. Slight departures from Lambertian behavior were observed at angles of incidence of 45 and 60°, although the surfaces were still highly diffuse.

MEASUREMENTS AND RESULTS

The following samples were available for the present study:

1. Flowers of sulfur, also known as sublimed sulfur powder. The sample was prepared by mixing the powder with acetone and compressing it in a tray, according to the "sulfur flooded" method described by Haner and Menzies.[5] The sample had a diameter of 5 cm.
2. Gold-coated sandpaper. This surface was available from previous studies at the Optical Sciences Center and was described by Stuhlinger *et al.*[6] A sample of 600 grit gold-coated sandpaper of 5 cm dia. was used.
3. A "certified reflectance standard" obtained from Labsphere (North Sutton, NH) of 5 cm dia., No. IRS-94-020. This consisted of a coarse sandblasted, gold electroplated surface.

†On שבתון (sabbatical leave) from the Technion-Israel Institute of Technology, Haifa, Israel.